Handling Technology of Mega-Watt Millimeter-Waves For Optimized Heating of Fusion Plasmas

Takashi Shimozuma[1*], Shin Kubo[1], Yasuo Yoshimura[1], Hiroe Igami[1], Hiromi Takahashi[1], Yasuyuki Takita[1], Sakuji Kobayashi[1], Satoshi Ito[1], Yoshinori Mizuno[1], Hiroshi Idei[2], Takashi Notake[3], Michael A. Shapiro[4], Richard J. Temkin[4], Federico Felici[5], Timothy Goodman[5], Olivier Sauter[5], Ryutaro Minami[6], Tsuyoshi Kariya[6], Tsuyoshi Imai[6] and Takashi Mutoh[1]

[1] National Institute for Fusion Science, 322-6 Oroshi-Cho, Toki-City, Gifu 509-5292 Japan
[2] Research Institute for Applied Mechanics Kyushu University, Kasuga, Fukuoka 816-8580, Japan
[3] Research Center for Development of Far-Infrared Region, University of Fukui, Fukui 910-8507, Japan
[4] Plasma Science and Fusion Center, Massachusetts Institute for Technology, Cambridge, MA 02139, USA
[5] Centre de Recherches en Physique des Plasma, EPFL-PPB, CH-1015, Lausanne, Switzerland
[6] Plasma Research Center (PRC), University of Tsukuba, Tsukuba 305-8577, Japan
[*] *shimozuma.takashi@LHD.nifs.ac.jp*

Millimeter-wave components were re-examined for high power (Mega-Watt) and steady-state (greater than one hour) operation. Some millimeter-wave components, including waveguide joints, vacuum pumping sections, power monitors, sliding waveguides, and injection windows, have been improved for high power CW (Continuous Waves) transmission. To improve transmission efficiency, information about the wave phase and mode content of high power millimeter-waves propagating in corrugated waveguides, which are difficult to measure directly, were obtained by a newly developed method based on retrieved phase information. To optimize the plasma heating efficiency, a proof-of-principle study of the injection polarization feedback control was performed in the low power test stand.

Submission Date: 8 September 2008
Acceptance Date: 27 February 2009
Publication Date: 30 May 2009

INTRODUCTION

Heating of plasma electrons based on Electron Cyclotron Resonance (ECRH) by Mega-Watt millimeter-waves (100 Giga-Hertz range) is promising for magnetic-confinement-fusion devices designed for nuclear fusion reactors. For example, to start the ITER (International Thermonuclear Experimental Reactor), a heating power above 20 MW with a frequency of 170 GHz and a pulse duration of 500 sec is required [Sakamoto *et al*., 2007]. In the Large Helical Device (LHD) of the National Institute for Fusion Science (NIFS) [Motojima *et al*., 1999], which employs superconducting

Keywords: *Millimeter-waves, Electron Cyclotron Resonance Heating, Corrugated waveguide, Phase retrieval, Polarizer*

Guest Editor: *Dr. Anish Upadhyaya, Indian Institute of Technology, Kanpur, India*

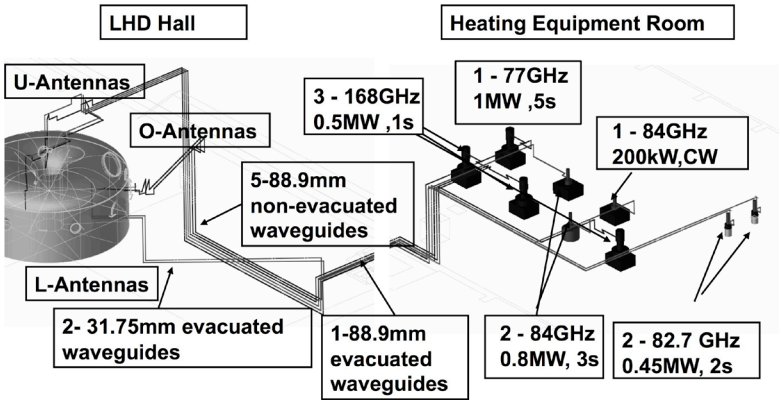

Figure 1. *Recent ECRH system in LHD. Nine gyrotrons are working.*

external magnets to produce magnetic fields for plasma confinement, numerous extensive plasma experiments have been carried out since 1998. An ECRH system consists of 8-9 high power gyrotrons, which realize high electron temperatures above 10 keV and a non-inductive current drive by EC waves [Shimozuma *et al*., 2006]. To date, the total injection power has exceeded 2 MW.

From a technological point of view, efficient plasma heating requires not only low-loss transmission of MW power in the steady state over a long distance, but focusing of millimeter-wave beams at the expected position with optimized wave polarizations given the injection angles and shape profiles of the power density. For this purpose, we have continuously upgraded our ECRH system; for example, we have developed high power CW gyrotrons, dummy loads, millimeter-wave beam shaping and focal position control by quasi-optical techniques, improved transmission efficiency, and transmitted power. In addition, we have studied alignment methods for long distance transmission lines, analyzed mode-content in the waveguide, and developed real-time feedback control of wave polarization to be injected. Herein, we overview technological aspects to handle the Mega-Watt level power of millimeter-waves for fusion plasma applications.

ECRH SYSTEM IN LHD

The ECRH system in LHD was upgraded in a stepwise manner at the beginning of the plasma experiments in LHD. Figure 1 summarizes recent ECRH system constituents, including gyrotrons, transmission lines and antennas. The ECRH system consists of nine-gyrotron systems (one 77 GHz/1 MW/5 sec, two 82.7 GHz/0.45 MW/2 sec, two 84 GHz/0.8 MW/3 sec, one 84 GHz/0.2 MW/CW, and three 168 GHz/ 0.5 MW/1 sec). Although numerous types of gyrotrons, which have a diode or triode electron gun with or without a depressed collector exist, two types of high voltage power supplies have been prepared. One is a solid-state power supply for the 77 GHz, 84 GHz, and 168 GHz gyrotrons with depressed collectors. The other is a conventional power supply, which precisely regulates the beam voltage by a regulator tube. This power supply is used for the two 82.7 GHz gyrotrons.

Figure 2 illustrates the typical configuration of a single line of the ECRH system with integrant components. The transmission line consists of matching optics units (MOU), over-sized corrugated waveguides, miterbends, waveguide switches, polarizers, arc detectors, power monitors, dummy loads, and an injection window. To evacuate the entire system, vacuum pumps and in-waveguide pumping sections are installed. The MOU includes two or four mirrors. In the two-mirror MOU, the mirrors quasi-optically correct the phase and power density profile as well as simultaneously align the millimeter-wave beam to the waveguide. In

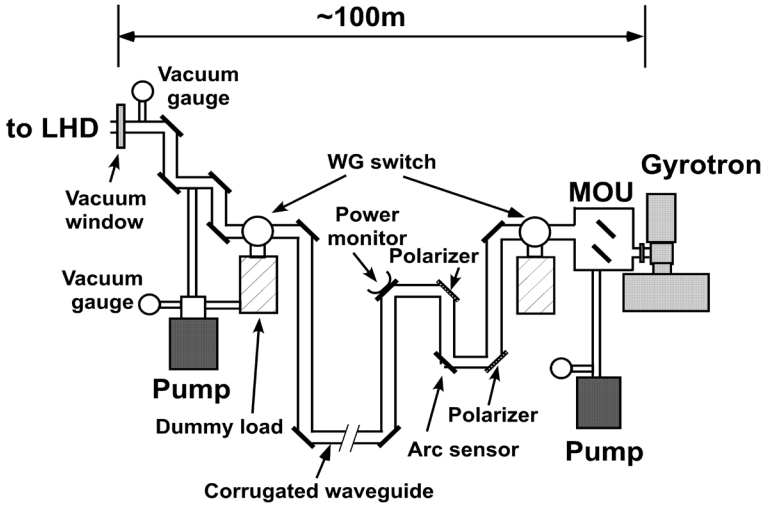

Figure 2. *Typical ECRH system, its configuration and some millimeter-wave integrant components.*

the four-mirror system, two are phase correcting mirrors and the others align the beam. High power millimeter-waves are transmitted through corrugated waveguides with diameters of 88.9 mm or 31.75 mm over a 100 m distance. Three transmission lines, one fat and two narrow waveguides, can be evacuated for higher power transmission capability.

In a few years, the ECRH system will be upgraded so that it is capable of 5 MW/10 sec and/or 1 MW/CW power injection into LHD. For this purpose, the system upgrade will be performed under the following strategies: First, the 77 GHz/1 MW gyrotrons will be installed progressively. Second, all the transmission lines will be evacuated for high power transmission to reassess all the transmission components. Third, the transmission components will be sufficiently cooled for CW operation. Fourth, the efficiency of the wave transmission will be improved not only to increase usable power, but also to avoid component overheating. Precise waveguide alignment is required to reduce transmission loss and mode conversion to unfavorable modes. Finally, the efficiency of plasma heating will be improved by real-time control of the heating position and polarization of injected waves.

Installation of 77 GHz/1 MW Gyrotrons

In collaboration with the University of Tsukuba, we have promoted the installation of high power 77 GHz gyrotrons (1-1.2 MW/5-10 sec, 300 kW/CW). These gyrotrons have been developed using the same technologies as that for the 170 GHz gyrotrons for ITER [Sakamoto *et al*., 2007]. Table 1 summarizes the specifications of the recent 77 GHz gyrotron. The selected oscillation mode is $TE_{18,6}$, which should have a total output efficiency above 50% with a depressed collector. The electron gun is a triode type, and due to its low loss-tangent and high thermal conductivity, the material of the output window is CVD diamond. The profile of the output power from the gyrotron is nearly a Gaussian profile, which is formed by an internal mode convertor and phase correcting mirrors. Figure 3 shows the installed 77 GHz gyrotron with beam sweeping coils into a super-conducting magnet.

Improvement of Typical Components in High Power Transmission Lines

For millimeter-waves, certain quasi-optical components such as mirrors can be used because of their short wavelength relative to the size of the components. To adequately introduce

Table 1. Specification of 77 GHz gyrotron.

Frequency	77 GHz ±0.2 GHz
Output power	1.2 MW 0.3 MW
Pulse width	10s CW
Total efficiency	50%
Beam voltage	80kV (Collector Voltage <65kV)
Beam current	< 50A
Electron gun	Triodes
Oscillation mode	TE18, 6
Output window	Diamond
RF output	Gaussian
Collector	CPD with Sweeping Coils
Height	3.1 m
Weight	~800 kg

high power millimeter-waves generated in a gyrotron into a corrugated waveguide over long distances with low transmission loss, one of the most important components is the MOU. Figure 4 shows a typical MOU with two phase-correcting mirrors, which is used in the 77 GHz transmission line. The mirrors are adjustable and water-cooled for CW operation. The inner surface of the MOU is coated with an absorbing material (TiO_2) in order to attenuate the diffracted RF fields and be cooled by water.

For long distance transmission of high power (1 MW level) and CW (greater than one hour) millimeter-waves, we have re-examined all transmission components to avoid arcing and overheating. Hence, the transmission line has been evacuated and sufficiently water-cooled because the transmission loss in this line was experimentally evaluated to be about 25% for 168 GHz. Evacuating the line reduces the occurrence of arcings at the high power level. For example, the maximum transmitted power level was limited to ~300 kW for a corrugated waveguide with an 88.9 mm diameter in air. After evacuating the line, over 800 kW of power could be transmitted without arcings. With regard to cooling the components, even 100 kW of power transmission causes the temperature to rise over 100 degrees throughout the transmission line without water-cooling the corrugated waveguides themselves. In the experiments of steady-state plasma sustainment in LHD, after 756 second transmission, the temperature rise resulted in a vacuum leak in the transmission line due to deformation of the waveguide and burning of resin materials. However, upon sufficient water-cooling of the waveguides and certain other components,

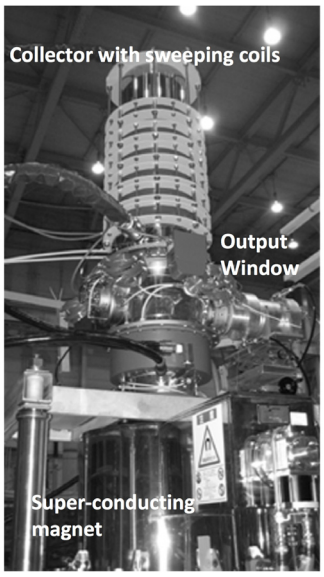

Figure 3. *77 GHz gyroton installed in the super-conducting magnet.*

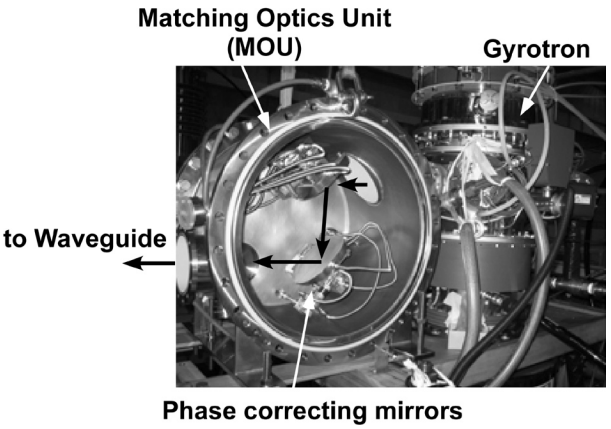

Figure 4. *Matching optics unit (MOU) with phase correcting mirrors and gyrotron.*

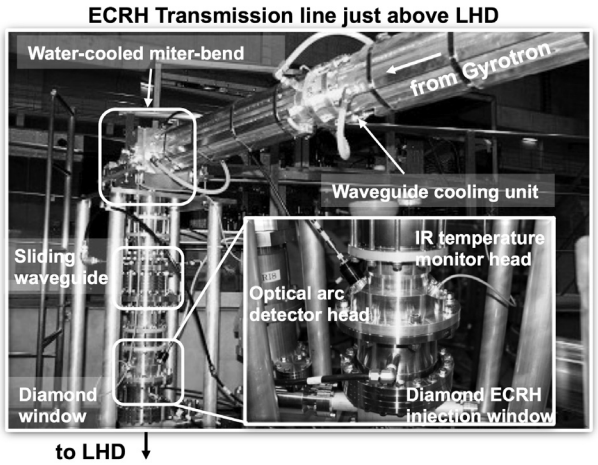

Figure 5. *Transmission lines and some millimeter-wave components.*

transmission at the same power level for 65 min could be achieved with a saturated temperature rise of the waveguides. Figure 5 is a photograph of the final section of the 77 GHz transmission line just above LHD where the miterbends, polarizers, power monitors, and corrugated waveguides are water-cooled. Especially, the waveguides equip water-cooling units along the entire line. A sliding waveguide has been installed in the straight section of the waveguide to adjust the position as well as to compensate the change in the length by thermal expansion. The structure of the waveguide joints and power monitors have been reconsidered and modified because the original ones could not be used in a vacuum. These components are equipped with as few rubber or plastic parts as possible for vacuum sealing to avoid burning by microwave absorption. When rubber O-rings are necessary, they are installed in places not directly irradiated by millimeter-waves. The final ECRH injection window has a CVD diamond disk as well as a gyrotron output window. The surface of the diamond disk in the injection window is monitored by an optical arc detector as well as an infrared temperature monitor to detect sudden arcings and unexpected heating.

Waveguide Alignment and Mode Analysis

In over-sized corrugated waveguides, the transmitted mode of HE_{11} can easily be converted to unwanted modes by tilting and offsetting the waveguide axis. Improving the transmission efficiency is essential in view of not only the increase in usable power, but also the reduction of the heat load to the millimeter-wave components. For example, to suppress a mode conversion loss to less than 1%, the tilt angle and offset of the beam center should be less than 0.1 deg. and 2.9 mm, respectively, for the 168 GHz transmission through a corrugated waveguide with a diameter of 88.9 mm [Ohkubo *et al*., 1997].

We have been researching an alignment method for high power millimeter-waves to corrugated waveguides based on infrared (IR) images on a target irradiated by high power millimeter-waves [Kuznezov *et al*., 1991, Shimozuma *et al*., 2005]. One method is based on phase information, which is sensitive to the propagating wave characteristics. This phase retrieval method has been used to obtain phase information because the phase of high power millimeter-waves cannot be measured directly. This method employs only wave intensity measurements in a few cross-sections, and is based on an iterative convergence procedure for phase reconstruction. It was originally developed by a Russian group on the basis of the calculation of the Huygens-Kirchhoff integral and has been compared to the other

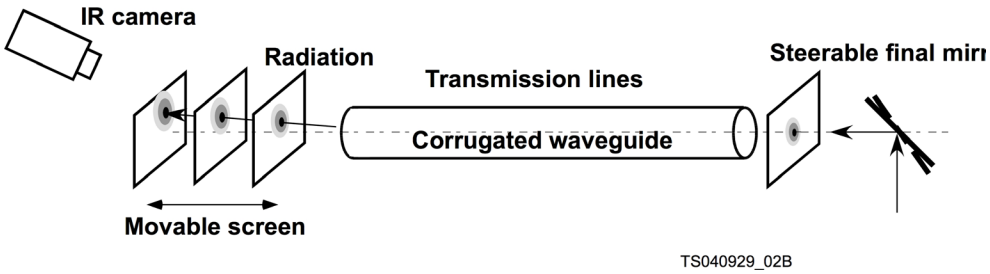

Figure 6. *Basic idea of phase retrieval and mode-content analysis.*

method [Chirkov *et al*., 1995; Chirkov *et al*., 2000; Antipov, 2003].

Figure 6 illustrates the basic idea of the alignment method based on the phase retrieval method. The transmission line, which consists of corrugated waveguides, should initially be aligned by a visible laser beam. After the millimeter-wave beam is coupled into the corrugated waveguide and propagated through the guide, it is irradiated to a target plate, which is set at a certain location away from the waveguide exit. An IR camera recorded the increase in temperature of the target. The measurements were repeated at the different target locations. Phase information, which provides precise information on the propagation direction, could be retrieved from the data [Shapiro *et al*., 2001]. The beam is then re-aligned according to the obtained information. As a next step, it is important to identify the propagating mode content in corrugated waveguides in order to clarify what type of misalignment induces such a mode conversion. Using the phase retrieval method, we can determine the complex amplitude at the radiating edge of the corrugated waveguide, which can be decomposed by the eigenmodes in the corrugated waveguide. The expansion coefficients by the eigenmodes give the mode content of the corresponding eigenmodes [Aleksandrov *et al*., 1997].

This method was applied to the 168 GHz transmission line in the ECRH system of LHD. The analyzed results show that the HE_{11} main propagating mode dominates (89%) and other spurious modes are HE_{21}/1.1%, HE_{12}/0.9% (even-mode) and HE_{21}/5.4%(odd-mode). Table 2 summarizes the analyzed mode content. The first moment of the radiation pattern, which represents the center of the power profile, is offset about 6 mm in the vertical direction, which partly explains the ratio of the HE_{11} mode content. The electromagnetic field in the waveguide can also be reconstructed by the expansion coefficients of these modes [Shimozuma *et al*., 2008]. Electric field reconstruction indicates that this offset is due to the 0.3 degree inclination of the beam axis to the waveguide axis at the waveguide entrance. In this case, the mode conversion from HE_{11} to the other modes becomes 7%.

Polarization Control for Optimized Heating

An effective ECRH requires the appropriate wave polarization, which is characterized by polarization angle, α, and the ellipticity, β,

Table 2. Summary of analyzed mode contents.

Mode	Even	Odd
HE11	88.841	-
HE12	0.910	-
HE13	0.158	-
HE14	0.118	-
HE15	0.161	-
HE21	1.149	5.357
HE22	0.140	0.684
HE23	0.079	0.131
HE24	0.012	0.086
HE25	0.036	0.177
HE31	0.432	0.048
HE41	0.147	0.021

at the plasma boundary, and depends on the injection mode and injection angle. As shown in Figure 7(a), α is the angle of the longer axis of the polarization ellipse formed with respect to the x-axis, which is the direction of the magnetic line of force at the plasma boundary, for example. The parameter β indicates the ellipticity of the polarization. The polarization state of the injected wave is usually controlled by a pair of rotatable corrugated reflectors ($\lambda/4$ and $\lambda/8$ plates) installed at the miterbends shown in Figure 2 [Doane, 1992; Nagasaki *et al*., 1995]. Figure 7(b) illustrates a polarizer system consisting of one rotatable grooved mirror. Generally a wave beam is injected on the grooved mirror with an incident angle of θ, which is normally 45 degrees in a miterbend. Adjusting the rotation angle of the mirror, ϕ, changes the direction of corrugation. The electric field components of the reflected wave are related to those of the incident wave by θ, ϕ and a phase delay, τ, as follows:

$$\begin{pmatrix} E_{r\phi} \\ E_{r\theta} \end{pmatrix} = \begin{pmatrix} -\cos(\tau/2) + i\sin(\tau/2)\cos(2\xi) & i\sin(\tau/2)\sin(2\xi) \\ -i\sin(\tau/2)\sin(2\xi) & \cos(\tau/2) + i\sin(\tau/2)\cos(2\xi) \end{pmatrix} \begin{pmatrix} E_{i\phi} \\ E_{i\theta} \end{pmatrix} \tag{1}$$

where $\xi=\tan^{-1}(\cos\theta\tan\phi)$. The electric field vector of the incident and reflected waves is decomposed into a component of the incident plane, E_θ and a component at a right angle to it, E_ϕ. The parameter, τ, represents the difference of the phase-shift between the parallel and perpendicular components of the electric vector with respect to corrugation after reflection. τ depends on the corrugation period, p, and depth, d, shown in Figure 7(c) and the angles, θ and ϕ. Practically, ϕ is the only variable for the parameter, τ, in the polarizer used in an actual ECRH system. τ is approximately represented by the Fourier series of ϕ by the following

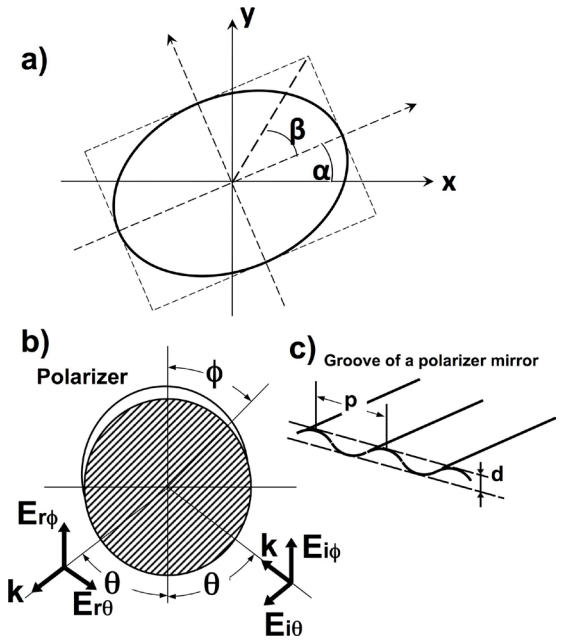

Figure 7. *Notation of polarization state and schematic configuration of the grating polarizer. a) the definition of polarization angles, ϕ and θ. b) a schematic drawing of one grating polarizer injected a millimeter wave beam. c) a structure and parameters of the grooved mirror.*

equation and the coefficients from m_0, m_1, m_2 ….. are numerically calculated for both $\lambda/4$ and $\lambda/8$ corrugated reflectors.

$$\begin{aligned} \tau = {} & m_1\cos\left[2(\phi+\pi/2)\right] + m_2\left[4(\phi+\pi/2)\right] \\ & + m_3\cos\left[6(\phi+\pi/2)\right] + m_4\cos\left[8(\phi+\pi/2)\right] \\ & + m_5\cos\left[10(\phi+\pi/2)\right] \end{aligned} \tag{2}$$

In the case of a system consisting of two polarizer mirrors, such as $\lambda/4$ and $\lambda/8$ corrugated reflectors, the matrix operation should be repeated using the reflected wave beam parameters as the next incident wave parameters.

Because the optimal polarization likely changes during a plasma discharge according to the change in plasma density at the boundary and the change in the boundary position itself, feedback control for the injected wave polarization

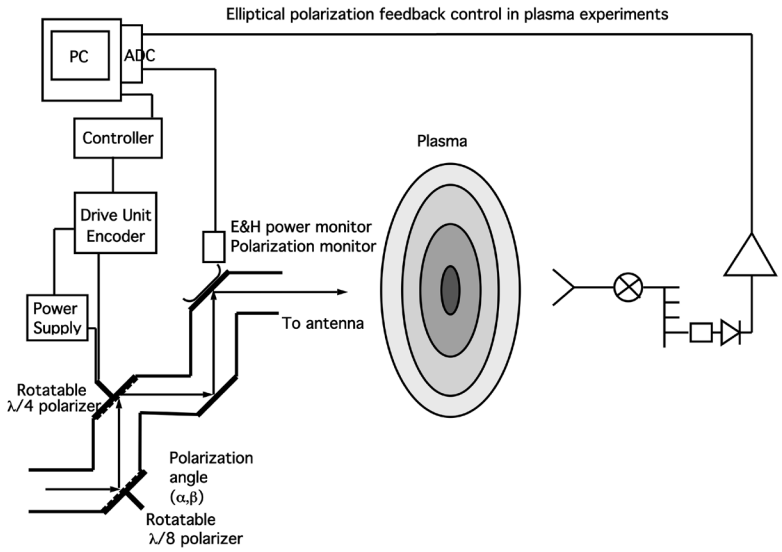

Figure 8. *Polarization feed back control system.*

during a single pulse becomes important to determine the maximum wave absorption. We have planned a feedback control system for the injected wave polarization, which corresponds to the response of the plasma electron temperature. Figure 8 conceptually illustrates the feedback control. The electron temperature at the plasma core, which can be obtained by the electron cyclotron emission measurement, is acquired and digitalized by a fast AD convertor and a computer. Then depending on electron temperature, the polarizer mirrors are rotated to maximize the electron temperature. The polarization state should be measured by the polarization monitor.

A proof-of-principle study has been performed with a pair of corrugated mirrors and crystal detectors in the low power millimeter-wave test stand, and a real time polarization monitor has been developed in collaboration with CRPP group of Lausanne, Switzerland [Felici *et al*.]. Figure 9 schematically illustrates the test stand. Millimeter-waves of 84 GHz are generated by a Gunn oscillator and radiated by a standard horn antenna. Two polarizer mirrors (λ/4 and λ/8 corrugated reflectors) are installed on rotating stages, which were set 45 degrees from the millimeter-wave beams. These rotating stages are controlled by a computer via GPIB (IEEE-488; General Purpose Interface Bus). The developed polarization monitor consists of a circular corrugated horn antenna, an ortho-mode transducer, two harmonic mixers, and an amplitude and phase detector (Analog devices AD8302), and outputs voltages proportional to the amplitude ratio and the phase difference of two orthogonal components of the received waves. Figure 10(a) is a block diagram of the polarization monitor, while Figure 10(b) plots the ideal outputs of AD8302, amplitude and phase. The output voltage, Vg, which corresponds to the ratio of two amplitudes, changes from 0 to 1.8 V according to the amplitude ratio, G, $G=20\times\log_{10}(E_\phi/E_\theta)$. The output of the phase difference, Vp, also changes from 0 to 1.8 V according to the phase difference, δ, $\delta = \arg\left(E_\phi E_\theta^* / \left|E_\phi\right|\left|E_\theta\right|\right)$. Hence, the intermediate frequency is ~700 MHz.

Figure 11 shows photographs of a) the low power test stand and b) the polarization monitor system. The polarization monitor has been tested in the low power test stand, and the dependence of output from AD8302 on the angles of the two polarizer plates has been measured and compared to the calculated results based on the equation (1). Figure 12 maps the output voltages from AD8302 on the angles of the two polarizer plates, Phi1 and

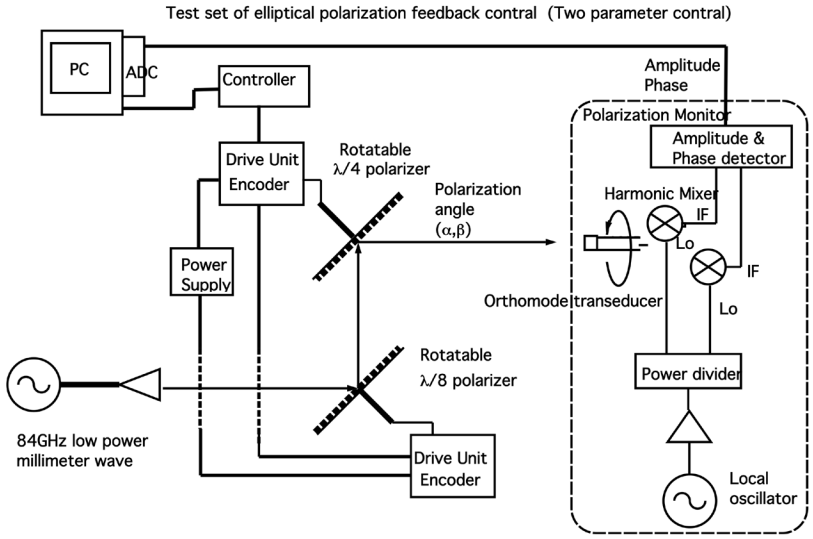

Figure 9. *Schematic diagram of polarization feedback control system for proof-of-principle study in the low power test stand.*

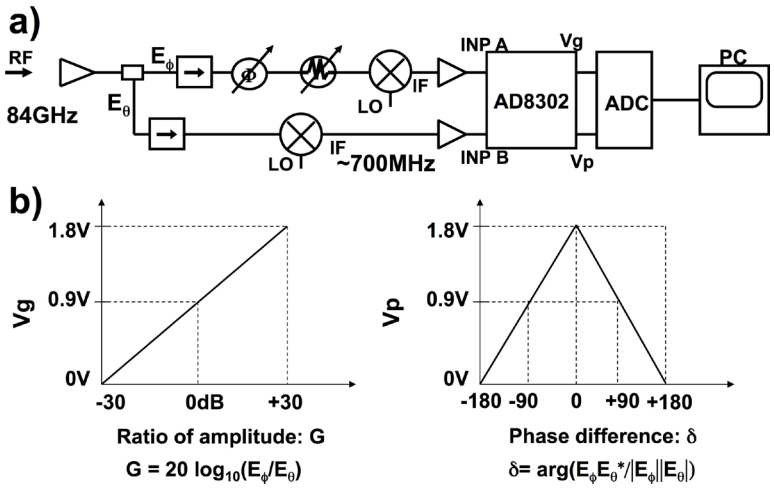

Figure 10. *a) Block diagram of a developed polarization monitor. b) The ideal output voltages of a gain and phase detector AD8302.*

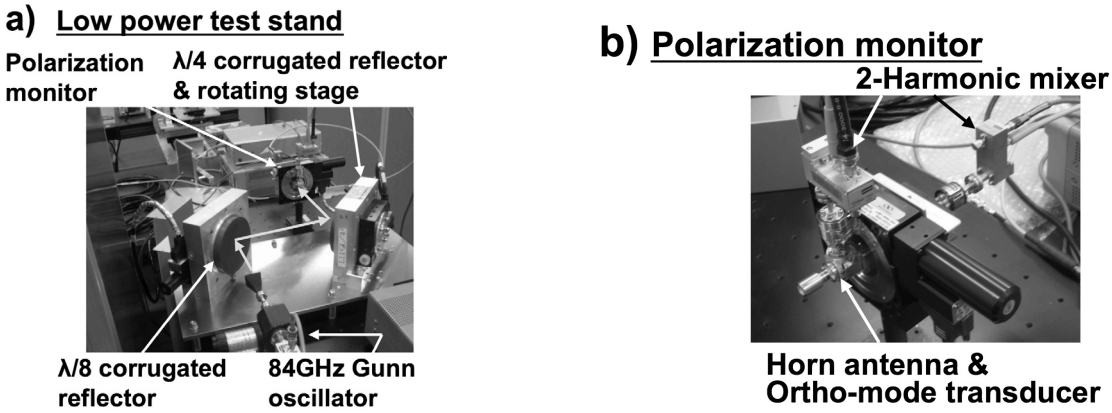

Figure 11. *a) photograph of the low power test stand, and b) polarization monitor.*

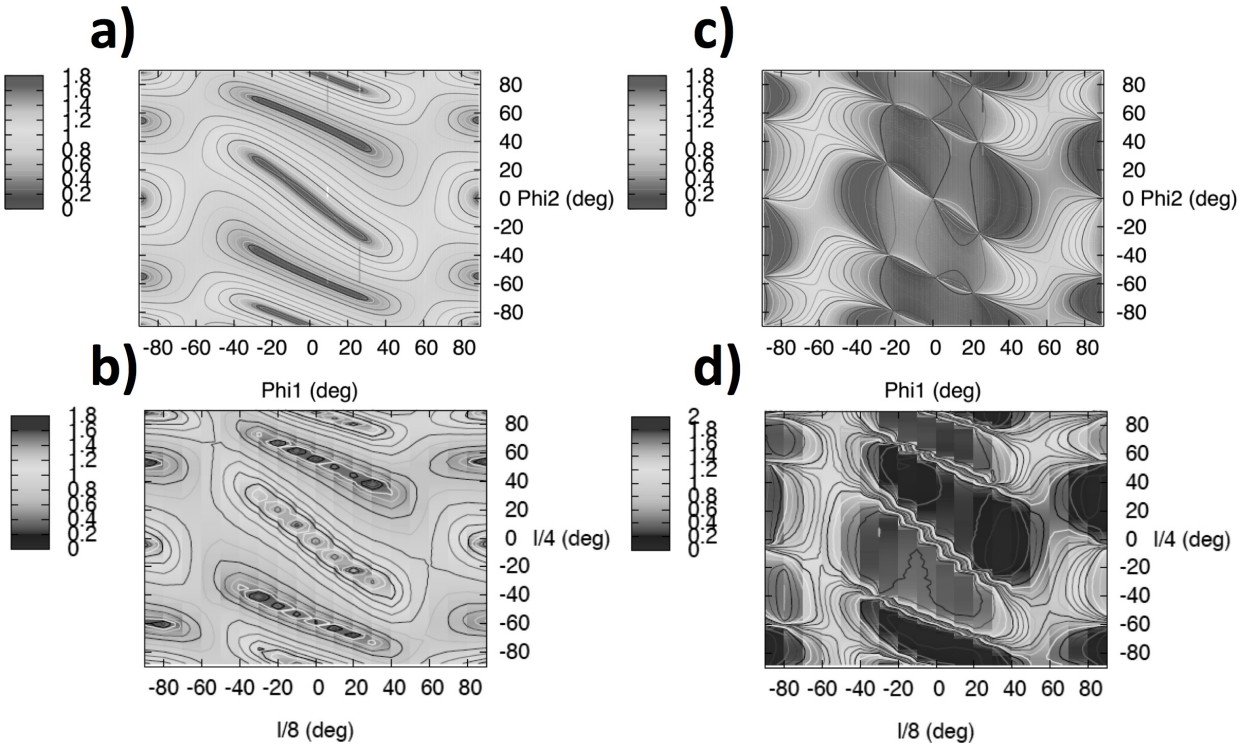

Figure 12. *a) calculated results of output voltages for gain; c) the phase differences are mapped on the angles of two polarizer plates. Phi1and Phi2 correspond to the angles of λ/8 and λ/4 corrugated plates, respectively. Corresponding measured results of output voltages for gain in b) and the phase difference in d) are also mapped on the Phi1 and Phi2 plane.*

Phi2, where Phi1 and Phi2 correspond to the angles of the λ/8 and λ/4 polarizer plates, respectively. The measured and calculated results agree well. Because the maximum speed of the rotating stage, which limits the speed of the feedback control, has been limited to 2 degrees/sec until now, the control system will be applied to plasma experiments with slow temperature and density changes, such as long time discharges by ECRH.

SUMMARY

The millimeter-wave components must be re-examined for high power (Mega-Watt) and steady-state (greater than one hour) operations. Thus, we have been improving select millimeter-wave components, including the matching optics unit, waveguide joints, power monitors, sliding waveguides, and injection window, for fusion plasma heating. Our efforts have focused on evacuating the entire system to avoid dangerous arcings and to sufficiently cool each component while improving its structure. To reduce the transmission loss, a new alignment method and mode-content analysis have been developed. The phase information obtained only from the measured intensity profiles can be used for mode-content analysis in corrugated waveguides, and may provide insight on aligning transmission lines. A real-time monitor and a feedback control system of the polarization state of the high power millimeter-waves have been developed, and their performances were evaluated at a low power level. The test results of the real-time polarization monitor agree well with the expected results based on theoretical calculations. These technologies will greatly contribute to high power millimeter-wave applications in other fields, including physical, chemical, biological, and industrial fields.

ACKNOWLEDGMENTS

The authors gratefully acknowledge Professors A. Komori, S. Sudo, and O. Motojima for their continuous guidance and encouragement. This work has been supported by NIFS under NIFS07ULRR501, 502, 503, and Grant-in-Aid for Scientific Research (C) 19560051. This work is also supported by NIFS/NINS under the project of Formation of International Network for Scientific Collaborations.

REFERENCES

Aleksandrov, N. L. , A. V. Chirkov, G. G. Denisov and S. V. Kuzikov (1997). "Mode Content Analysis from Intensity Measurements in a Few Cross Sections of Oversized Waveguides." *Int. J. Infrared and Millimeter Waves*, 18, pp.1505.

Antipov, S. P., A. A. Bogdashov, A. V. Chirkov and G. G. Denisov (2003). "Comparison of Wavebeam Phase Front Retrieval Methods Besed on Iterative Algorithm and Irradiance Moments." *Int. J. Infrared and Millimeter Waves*, 24, pp.1677.

Chirkov, A. V., G. G. Denisov, N. L. Aleksandrov (1995). "3D Wave Beam Field Reconstruction from Intensity Measurements in a Few Cross Sections." *Optics Communications*, 115, pp.449.

Chirkov, A. V. and G. G. Denisov (2000). "Methods of Wavebeam Phase Front Reconstruction Using Intensity Measurements." *Int. J. Infrared and Millimeter Waves*, 21, pp.83.

Doane J. L. (1992). "Grating Polarizers in Waveguide Miter Bends." *Int. J. Infrared and Millimeter Waves*, 13, pp.1727.

Felici, F. T., Goodman, O. Sauter, T. Shimozuma, S. Ito, Y. Mizuno, S. Kubo, and T. Mutoh (2009). "Real-Time Feedback Control of Millimeter-wave Polarization for LHD." *Rev. Sci. Instrum.*, 80, 013504.

Kuznezov, S. O., and V. I. Malygin (1991). "Determination of Gyrotron Wave Beam Parameters." *Int. J. Infrared and Millimeter Waves*, 12, pp.1241.

Motojima, O., H. Yamada, A. Komori, N. Ohyabu, K. Kawahata, O. Kaneko, et al. (1999). "Initial Physics Achievements of Large Helical Device Experiments." *Physics of Plasmas,* 6, pp.1843.

Nagasaki, K., A. Isayama, and A. Ejiri (1995). "Application of a Grating Polarizer to the 106.4GHz ECH System on Heliotron-E." *Rev. Sci. Instrum,*. 66, pp.3432.

Ohkubo K., S. Kubo, H. Idei, M. Sato, T. Shimozuma and Y. Takita (1991). "Coupling of Tilting Gaussian Beam with Hybrid Mode in the Corrugated Waveguide." *Int. J. Infrared and Millimeter Waves* 18, pp.23.

Sakamoto, K., A. Kasugai, K. Takahashi, R. Minami, N. Kobayashi, and K. Kajiwara (2007). "Achievement of Robust High-Efficiency 1 MW Oscillation in the Hard-Self-Excitation Region by a 170 GHz Continuous-Wave Gyrotron." *Nature Physics,* 3, pp.411.

Shapiro, M. A., T. S. Chu, D. R. Denison, M. Sato, T. Shimozuma, and R. J. Temkin (2001). "Design of Correcting Mirrors for a Gyrotron used at large Helical Device." *Fusion Engineering and Design,* 53, pp.537.

Shimozuma, T., H. Idei, M. Shapiro, R. Temkin, S. Ito, T. Notake, S. Kubo, Y. Yoshimura, S. Kobayashi, Y. Mizuno, Y. Takita and K. Ohkubo (2005). "Alignment Method of ECH Transmission Lines Based on the Moment and Phase Retrieval Method Using IR Images." *J. Plasma and Fusion Research,* 81, pp.191.

Shimozuma, T., S. Kubo, Y. Yoshimura, H. Igami, K. Nagasaki, T. Notake, S. Inagaki, et al.(2006). "Progress on Electron Cyclotron Heating and Electron Cyclotron Current Drive Experiments in LHD." *Fusion Science and Technology,* 50, pp.403.

Shimozuma, T. H. Idei, M.A. Shapiro, R. J. Temkin, S. Kubo, H. Igami, Y. Yoshimura, H. Takahashi, S. Ito, S. Kobayashi, Y. Mizuno, Y. Takita and T. Mouth (2008). "Analysis of Propagating Mode Contents in the Corrugated Waveguides of ECH System for Precise Alignment." P*roc. on the 18th International Toki Conference* (ITC18), P2-02, Toki, Japan, Dec. 9-12, 2008.